BIOPHYSICS

Precise control of synthetic hydrogel network structure via linear, independent synthesis-swelling relationships

N. R. Richbourg[1,2], M. Wancura[3], A. E. Gilchrist[4], S. Toubbeh[1], B. A. C. Harley[5,6,7], E. Cosgriff-Hernandez[1], N. A. Peppas[1,2,8,9,10]*

Hydrogel physical properties are tuned by altering synthesis conditions such as initial polymer concentration and polymer–cross-linker stoichiometric ratios. Traditionally, differences in hydrogel synthesis schemes, such as end-linked poly(ethylene glycol) diacrylate hydrogels and cross-linked poly(vinyl alcohol) hydrogels, limit structural comparison between hydrogels. In this study, we use generalized synthesis variables for hydrogels that emphasize how changes in formulation affect the resulting network structure. We identify two independent linear correlations between these synthesis variables and swelling behavior. Analysis through recently updated swollen polymer network models suggests that synthesis-swelling correlations can be used to make a priori predictions of the stiffness and solute diffusivity characteristics of synthetic hydrogels. The same experiments and analyses performed on methacrylamide-modified gelatin hydrogels demonstrate that complex biopolymer structures disrupt the linear synthesis-swelling correlations. These studies provide insight into the control of hydrogel physical properties through structural design and can be used to implement and optimize biomedically relevant hydrogels.

INTRODUCTION

Hydrogels are polymer networks swollen in water or biological fluids that can be used in a range of biomedical applications such as drug delivery carriers (*1*), biosensors (*2*), and soft tissue scaffolds (*3*). The functional properties of a hydrogel originate from its structure at multiple length scales (*4*), with mounting evidence for the importance of physical properties in controlling biological behavior (*5*–*7*). Atomic-scale chemical structure of the polymeric repeating units and pendant functional groups control most of the hydrogel's chemical properties, and larger-scale features such as nanoscale mesh size, microscopic pores, and the overall polymer concentration primarily affect physical properties such as stiffness and solute transport (*8*).

The diversity of possible structures at each length scale facilitates a wide range of chemical and physical properties but hinders comprehensive analysis of structure-function relationships. Differences in the reaction schemes used to form polymer networks such as end-linked poly(ethylene glycol) diacrylate (PEGDA) hydrogels, midpoint-linked multi-arm PEG (mPEG) hydrogels, and glutaraldehyde–cross-linked poly(vinyl alcohol) (PVA) hydrogels complicate the relationship between polymer properties and network properties. For example, in both PEGDA hydrogels and mPEG hydrogels, increasing molecular weight contributes directly to the resulting network's molecular weight between cross-links, but in PVA hydrogels, the molecular weight primarily affects the frequency of chain-end defects and contributes negligibly to molecular weight between cross-links. Broadly applicable structure-based synthesis variables that address the similarities and differences in reaction schemes are needed to evaluate universal structure-function relationships.

Swollen polymer network models aim to fundamentally relate hydrogel structure to physical properties such as swelling, stiffness, and solute transport. In our recent review, we discussed how these models can be coordinated to predict stiffness and solute diffusivity from hydrogel swelling behavior (*9*). Reliable swelling-based prediction of stiffness and solute diffusivity would enable iterative synthesis and swelling characterization of hydrogels to attain desirable physical properties for targeted biomedical applications, which would be a practical improvement over heuristically guided trial-and-error synthesis with full physical characterization of each system. However, even iterative synthesis can be costly and inefficient, especially as hydrogels are formed from increasingly rare or expensive materials such as DNA (*10*), bioactive peptide sequences (*11*), or customized synthetic polymers (*12*). As hydrogel synthesis and properties become more advanced, a synthesis-to-swelling model that could interface with the swollen polymer network models to make a priori predictions of physical properties will become increasingly valuable. With this work, we aim to establish the fundamental principles of such a model in well-established polymer systems before expanding the approach to more advanced systems.

Here, we investigated the structural similarities between cross-linked and end-linked synthetic hydrogels using PVA hydrogels and PEGDA hydrogels. We observed independent, linear correlations between structurally defined synthesis conditions and precisely measured swelling ratios in both systems, suggesting a highly controllable relationship between structure and physical properties that was then validated using data interpreted from previous reports. We then used swollen polymer network models to estimate and compare molecular weight between cross-links, shear modulus, and mesh size for each hydrogel formulation. The synthesis, swelling, and modeling were repeated with a third system of methacrylamide–cross-linked gelatin, which did not replicate the linear synthesis-swelling behavior, demonstrating the current limitations of structural hydrogel design in biopolymer hydrogels.

[1]Department of Biomedical Engineering, University of Texas, Austin, TX 78712, USA. [2]Institute for Biomaterials, Drug Delivery, and Regenerative Medicine, University of Texas, Austin, TX 78712, USA. [3]Department of Chemistry, University of Texas, Austin, TX 78712, USA. [4]Department of Materials Science and Engineering, University of Illinois at Urbana-Champaign, Urbana, IL 61801, USA. [5]Department of Chemical and Biomolecular Engineering, University of Illinois at Urbana-Champaign, Urbana, IL 61801, USA. [6]Carl R. Woese Institute for Genomic Biology, University of Illinois at Urbana-Champaign, Urbana, IL 61801, USA. [7]Cancer Center at Illinois, University of Illinois at Urbana-Champaign, Urbana, IL 61801, USA. [8]McKetta Department of Chemical Engineering, University of Texas, Austin, TX 78712, USA. [9]Division of Molecular Therapeutics and Drug Delivery, College of Pharmacy, University of Texas, Austin, TX 78712, USA. [10]Departments of Surgery and Pediatrics, Dell Medical School, University of Texas, Austin, TX 78712, USA.
*Corresponding author. Email: peppas@che.utexas.edu

RESULTS AND DISCUSSION

Cross-validation of volumetric swelling methods

Before analyzing synthesis-swelling relationships, we validated the accuracy of swelling characterization using two independent methods for measuring the polymer volume fraction. The mass-based method obtains a polymer mass fraction by dividing the mass of the dried polymer network by its mass when swollen in solution and then calculating the polymer volume fraction using literature values for the density of the polymer and solution (Eqs. 8 to 11). Calculation of polymer volume fraction based on polymer mass fraction (or its inverse, mass swelling ratio) is common practice for hydrogel characterization studies (*13*–*15*). However, the mass-based method relies on the knowledge of polymer and solvent densities and the assumption of additive volumes. The buoyancy-based method, developed by Reinhart and Peppas (*16*), additionally weighs the hydrogel sample while submerged in a nonsolvent solution, using the volume-dependent buoyant force to determine polymer volume fraction without previous knowledge of polymer and solution densities (Eqs. 3 to 5). For each PVA and PEGDA hydrogel formulation studied in the following sections, the relaxed polymer volume fraction (φ_r; immediately following hydrogel synthesis) and swollen polymer volume fraction (φ_s; following swelling to equilibrium in excess solution) were measured using both methods.

Mass- and buoyancy-based measurements resulted in highly similar values of polymer volume fraction (Fig. 1), suggesting that the polymer densities used in the mass-based calculations are appropriate. The collinearity of the relaxed state and the swollen state values suggests that the soluble by-products from the hydrogel synthesis, which are present in the relaxed state but washed out while swelling to equilibrium, do not affect the component densities of the polymer or the solvent. The low SDs in the PVA and PEGDA formulations indicate that the buoyancy-based method results in precise measurements of polymer volume fraction. Polymer mass fractions measurements using the mass-based method were similarly precise, as indicated by the horizontal error bars, but the precision of the polymer volume fractions calculated using the mass-based method could not be determined directly without reliable SD information for the polymer densities.

In addition to measuring polymer volume fractions, the buoyancy-based method enables measurement of the density of the hydrogel in each state. All swollen or partially swollen (relaxed state) hydrogels had densities that were statistically indistinguishable from the density of water, consistent with the measured polymer volume fractions indicating that they were all more than 80% water by volume. However, dry densities of the polymer networks provided an interesting comparison with literature reports of the dry density for each polymer. PVA hydrogels, with a reported polymer density of 1.27 g/cm^3 (*17*), were found to have a polymer network dry density of 1.24 ± 0.01 (n = 103). PEGDA hydrogels, with a reported polymer density of 1.18 g/cm^3 (*13*), had a polymer network dry density of 1.20 ± 0.06 g/cm^3 (n = 180). Together, these results suggest that formation of a polymer network negligibly affects the dry polymer density.

From the comparative analysis of mass- and buoyancy-based determination of polymer volume fractions for PVA and PEGDA hydrogels, we found that the mass-based calculation may be broadly sufficient for synthetic polymer hydrogels with well-characterized polymer densities. However, for more complex systems such as interpenetrating network hydrogels, copolymer hydrogels, and biopolymer hydrogels, where density is not well characterized, the buoyancy-based method provides a highly accurate and polymer density–independent method for evaluating polymer volume fractions. Furthermore, the three-dimensional (3D)–printed density kit developed for this study (instructions included in Materials and Methods) makes the buoyancy-based method broadly accessible. For consistency and high precision within this report, all hydrogel polymer volume fractions used in the following sections were calculated using the buoyancy-based method.

Formulation-dependent swelling behavior of synthetic hydrogels

For each hydrogel system (PVA or PEGDA), a matrix of hydrogel formulations was synthesized by independently manipulating the initial polymer volume fraction (φ_0) and the expected degree of polymerization between cross-links (N_c). Initial polymer volume fraction corresponds to polymer concentration, often reported in literature as molar or mass ratios. In this investigation, initial polymer volume fractions are represented by the volumetric fraction to facilitate comparison with swelling measurements across polymer systems. The expected degree of polymerization between cross-links represents the number of polymeric repeating units between network junctions, facilitating structural comparison between cross-linked and end-linked

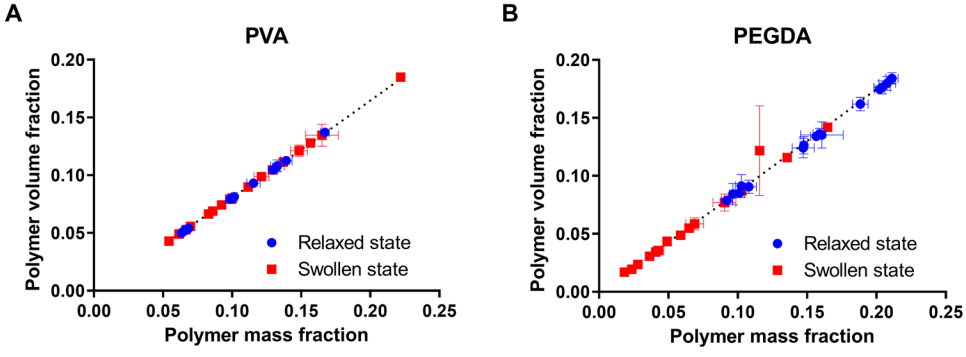

Fig. 1. Comparison of methods for measuring polymer volume fraction. Polymer volume fractions in the relaxed and swollen states were measured using the mass-based method and the buoyancy-based method for (**A**) PVA hydrogels and (**B**) PEGDA hydrogels. The dashed lines represent the conversion from polymer mass fraction to polymer volume fraction, which is a continuous function dependent on the polymer and solvent density ($\rho_{p,\,PVA}$ = 1.27 g/cm^3, $\rho_{p,\,PEGDA}$ = 1.18 g/cm^3, ρ_w = 1.00 g/cm^3). Buoyancy-based measurements of the hydrogels in the relaxed state and the swollen state are represented as points for each hydrogel formulation, with error bars representing SD across multiple samples. (A) PVA hydrogels (n = 6). (B) PEGDA hydrogels (n = 12).

hydrogel systems. The calculations for initial polymer volume fraction and expected degree of polymerization between cross-links are provided in Materials and Methods (Eqs. 1 and 2), and the synthesis conditions for each hydrogel formulation are listed in both structure-based and standard variables in the Supplementary Materials (tables S1 and S2).

For each formulation, swelling was initially measured and characterized as the relaxed polymer volume fraction and the swollen polymer volume fraction as described in the previous section. However, we hypothesized that the relaxed polymer volume fraction should not change from the initial polymer volume fraction. Mechanistically, this result would suggest that the cross-linking reaction and the formation of the network do not initially strain the polymer chains. To then isolate the effect of the expected degree of polymerization between cross-linking on swelling to equilibrium, we defined a new swelling variable, the reference ratio (θ), to describe how hydrogels swell from the relaxed state to the equilibrium-swollen state. The calculation for reference ratio is provided in Materials and Methods (Eq. 6). A reference ratio greater than one indicates swelling from the relaxed state, and a reference ratio less than one indicates expulsion of water from the system to reach equilibrium.

Separating the swollen polymer volume fraction into the relaxed polymer volume fraction and the reference ratio revealed independent linear relationships with the initial polymer volume fraction and the expected degree of polymerization between cross-links (Fig. 2). For PVA hydrogels, a global fit of all formulations showed a nearly one-to-one match of initial polymer volume fraction to relaxed polymer volume fraction ($\varphi_r = 1.17\varphi_0 - 0.0062$, $R^2 = 0.93$) (Fig. 2A). The relationship between initial polymer volume fraction and relaxed polymer volume fraction was independent of the expected degree of polymerization between cross-links except for a deviation at the lowest degree and high initial polymer volume fraction. The deviation, with the relaxed polymer volume fraction increasing nonlinearly with respect to the initial polymer volume fraction, suggests that syneresis occurred, which was confirmed visually. The PVA hydrogels with expected degree of polymerization of 20 and initial polymer volume fractions of 7.5 and 10% had droplets of expelled water on their surface following synthesis, unlike other formulations. Notably, all PVA hydrogel formulations were optically clear following synthesis, suggesting that the syneresis did not result from cross-linking–induced phase separation. We discuss plausible explanations for the syneresis at the end of this section. In PEGDA hydrogels, the relaxed polymer volume fraction closely matches the initial polymer volume fraction with no identifiable effects from the degree of polymerization between cross-links (Fig. 2B). The global linear fit for PEGDA was a precise one-to-one line ($\varphi_r = 1.01\varphi_0 - 0.0001$, $R^2 = 0.95$). Together, these results suggest that the initial polymer volume fraction independently controls the relaxed polymer volume fraction in synthetic polymer hydrogels. The one-to-one relationship suggests that the cross-linking reaction does not cause swelling or deswelling except in cases of extensive cross-linking, as observed in the PVA hydrogels.

The expected degree of polymerization between cross-links showed a strong linear correlation with reference ratio, independent of the initial polymer volume fraction (PVA: $\theta = 0.0090 * N_c + 0.53$, $R^2 = 0.95$; PEGDA: $\theta = 0.0085 * N_c + 0.57$, $R^2 = 0.91$) (Fig. 2, C and D). The syneresis seen in PVA hydrogels does not affect the relationship

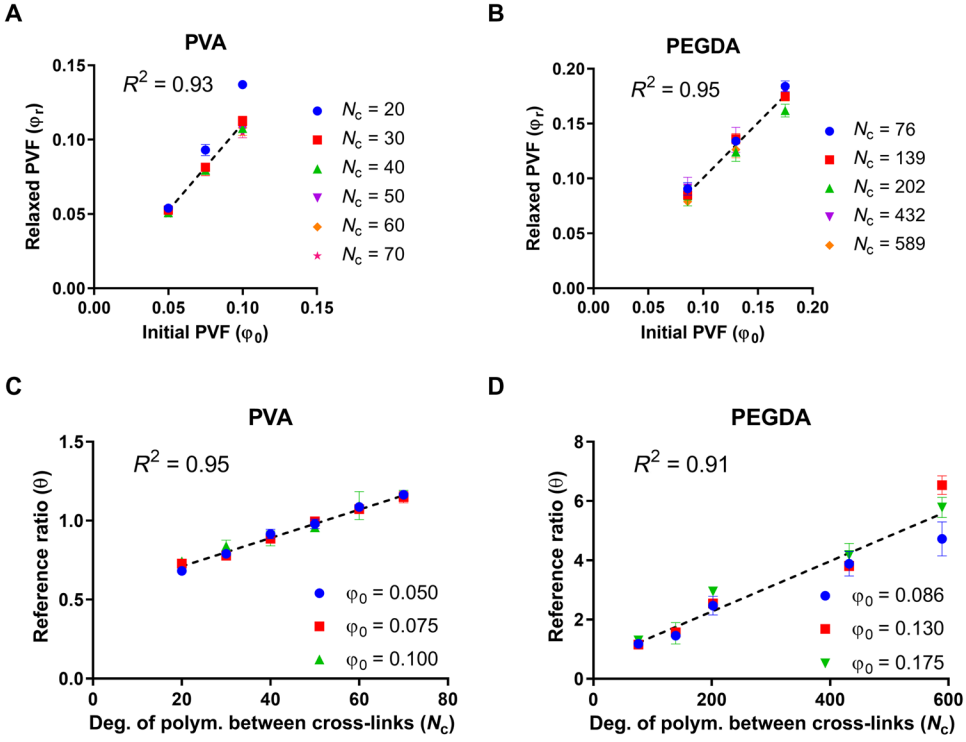

Fig. 2. Linear, independent correlations between synthesis conditions and swelling characteristics. Initial polymer volume fraction (φ_0) correlates to the relaxed polymer volume fraction (φ_r) in (**A**) PVA hydrogels and (**B**) PEGDA hydrogels. Expected degree of polymerization between cross-links (N_c) correlates to reference ratio (θ) in (**C**) PVA hydrogels and (**D**) PEGDA hydrogels. Dotted lines represent linear fits across all hydrogel formulations for each system with associated R^2 values displayed on each graph. Error bars represent SDs ($n = 6$ for PVA; $n = 12$ for PEGDA; $n = 4$ for GelMA).

between expected degree of polymerization between cross-links and reference ratio. Together, these results suggest that the expected degree of polymerization between cross-links linearly controls the reference ratio in synthetic polymer hydrogels, independent of the initial polymer volume fraction. Unexpectedly, while the correlation between expected degree of polymerization between cross-links and swelling is anticipated by the swollen polymer network model and mechanistically associated with the entropic spring behavior of polymer chains in a network (*9*), the experimentally observed independence from the initial polymer volume fraction is not. We discuss this model-experiment discrepancy in greater detail in the "Modeling molecular weight between cross-links" section.

With these synthesis-swelling experiments, we demonstrated that synthetic hydrogel swelling, as summarized by the equilibrium-swollen polymer volume fraction, can be precisely controlled by two independent structural synthesis variables. Initial polymer volume fraction controls the relaxed polymer volume fraction unless disrupted by extreme cross-linking, and the degree of polymerization between cross-links controls the extent of swelling from the relaxed polymer volume fraction to the swollen polymer volume fraction. No strong batch variability was observed in PVA and PEGDA hydrogels (fig. S1), and all linear fits with SDs and R^2 values are available in the Supplementary Materials (table S3). Mechanistically, the linear synthesis-swelling correlations suggest that the polymer chains within the network are unstrained following cross-linking, and the extent of swelling from that relaxed state in excess solution depends on the entropic spring-like behavior of uncoiling polymer chains. This relationship is presently validated on PVA and PEGDA hydrogels within the studied ranges of initial polymer volume fraction and degree of polymerization between cross-links. Possible limitations include loss of linearity as the polymer becomes concentrated enough for the polymer-solvent interaction parameter to change in response to the polymer volume fraction (*18*) or dilute enough to approach the critical gelation concentration, which would markedly reduce the efficiency of polymer chains incorporating into the network (*19*).

In addition to the two independent and linear synthesis-swelling relationships, two features of the PVA hydrogel swelling dataset require further consideration. First, there is the syneresis that exclusively affected the two most cross-linked and polymer-dense PVA hydrogel formulations, and the second feature is the reference ratios that are less than unity for highly cross-linked PVA hydrogels, indicating systematic deswelling from the relaxed state to reach equilibrium.

As discussed above, the syneresis only affected the two most highly cross-linked PVA hydrogel formulations and was not associated with phase separation. To explain why all formulations with $N_c = 20$ were not affected equally, we note that the total concentration of glutaraldehyde was highest in the 10% formulation (2.8% v/v 25% glutaraldehyde solution) and the 7.5% formulation (2.0% v/v 25% glutaraldehyde solution), with the third highest glutaraldehyde concentration in the 10%, $N_c = 30$ formulation (1.9% v/v 25% glutaraldehyde solution), which did not clearly deviate from the trend. The 5%, $N_c = 20$ formulation (1.3% v/v 25% glutaraldehyde solution) did not clearly deviate from the trend. These results suggest that the final concentration of 25% v/v glutaraldehyde solution should be kept below 2% to maintain linearity but do not clarify the mechanism behind the syneresis. We suggest that it might be a combination of marginal effects from the synthesis including cooling from the 90°C used to dissolve the PVA in solution as well as mixing inhomogeneity of the solution, PVA, and glutaraldehyde, all exacerbated by the high concentration of glutaraldehyde. High cross-linking concentrations, sometimes described as cross-linking densities, have been associated with skewed, non-Gaussian chain length distributions and chains too short to behave as ideal entropic springs (*9*, *20*, *21*), but it is unclear whether these formulations enter that regime, especially because the relationship between expected degree of polymerization between cross-links and reference ratio does not deviate from linearity with the highly cross-linked formulations. Further studies with nonspontaneous cross-linking reactions are needed to evaluate how high cross-linking causes deviation from a one-to-one initial polymer volume fraction to relaxed polymer volume fraction relationship.

The reference ratios of the PVA hydrogel formulations range from 0.68 to 1.16, showing a consistent capability for deswelling from the relaxed state, contrary to previous expectations of hydrogel swelling behavior. The PEGDA formulations did not deswell, but that may be because their expected degrees of polymerization between cross-links were not low enough to cause a reference ratio below one. Notably, in the next section, which meta-analyzes previous swelling data, PVA hydrogels and other hydrogel systems showed expected degree of polymerization between cross-linking–dependent deswelling (Fig. 3), so the effect is not isolated to our experimental approach or to PVA hydrogels. If we maintain the possibly limiting interpretation that the chains of the polymer network are unstrained in the relaxed state, then deswelling from that state will introduce compressive strain that must be matched by an inverted value of the mixing term to reach equilibrium. In effect, the mixing term would have to have a strong dependence on the degree of polymerization between cross-links, possibly through changes to the polymer-solvent interaction parameter. However, such a conclusion has not been presented before

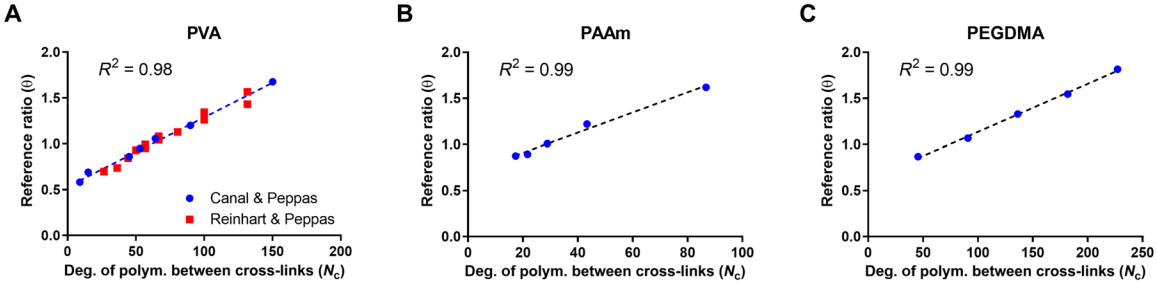

Fig. 3. Meta-analysis of the relationship between expected degree of polymerization between cross-links (N_c) and reference ratio (θ). Dotted lines represent linear fits across all hydrogel formulations for each system with associated R^2 values displayed on each graph. (**A**) Data for PVA hydrogels were taken from Canal and Peppas (*22*) and Reinhart and Peppas (*16*). (**B**) Data for PAAm hydrogels were taken from (*23*). (**C**) Data for PEGDMA hydrogels were taken from (*24*).

in the literature, and we cannot make this claim with certainty without further validating that rubberlike elasticity and Flory-Huggins entropic mixing are the only two contributions to equilibrium swelling in synthetic hydrogels. As we show in the "Modeling molecular weight between cross-links" section, degree of polymerization between cross-link–dependent deswelling to equilibrium is not the only experimental inconsistency with equilibrium swelling theory and modeling revealed by this study.

A major impact of these studies is the ability to apply the synthesis-swelling relationships described here to synthesize hydrogels with a targeted equilibrium swelling ratio. Equilibrium swelling ratio can be calculated by inverting the equilibrium-swollen polymer volume fraction or by taking the quotient of the reference ratio and the relaxed polymer volume fraction. In the following sections, we investigate whether the linear synthesis-swelling relationships apply to other hydrogel systems and how those relationships work together with swollen polymer network models to enable a priori prediction of stiffness and solute transport in hydrogels.

Meta-analysis of expected degree of polymerization between cross-links and reference ratio

To evaluate the broad applicability of trends observed in the experimental data, literature data were reanalyzed using the concepts of expected degree of polymerization between cross-links and reference ratio (Fig. 3). Because reporting of the relaxed polymer volume fraction is not yet common practice in hydrogel swelling characterization, the relationship between initial polymer volume fraction and relaxed polymer volume fraction was not analyzed. Instead, the reference ratio was approximated by substituting the initial polymer volume fraction for the relaxed polymer volume fraction and therefore dividing the initial polymer volume fraction by the swollen polymer volume fraction.

Two separate previous studies by Peppas and colleagues (*16*, *22*) demonstrated that the linear relationship between expected degree of polymerization between cross-links and reference ratio remains valid for PVA hydrogels over a wide range of degrees of polymerization between cross-links (Fig. 3A). Notably, the difference between the linear fits for the two datasets is not statistically significant, allowing a global linear fit ($\theta = 0.0075 * N_c + 0.53$, $R^2 = 0.98$). The literature-based linear fit has the same Y intercept as the experimental PVA data gathered in this study but a significantly different slope (0.0075 versus 0.0090; $P = 0.0002$). This difference may result from the nonparameterized differences in synthesis conditions between studies. Both previous studies used PVA with a number-average molecular weight of 52,800 g/mol, whereas the current study used PVA with a number-average molecular weight of 33,900 g/mol. In addition, the previous studies used sulfuric acid to catalyze the PVA-glutaraldehyde reaction and methanol as a quencher, whereas the current study simply created an acidic reaction environment by introducing hydrochloric acid to the solution. Together, these differences indicate that additional synthesis conditions may affect the relationship between expected degree of polymerization between cross-links and reference ratio.

In addition to previous studies on PVA hydrogels, literature data relating expected degree of polymerization between cross-links to the reference ratio in a variety of polymer systems were evaluated to validate whether the linear relationship was broadly applicable (Fig. 3, B and C). Polyacrylamide (PAAm) and PEG dimethacrylate (PEGDMA) hydrogels showed highly consistent positive correlations ($R^2 = 0.99$ for each system) (*23*, *24*). These data contribute to the argument that expected degree of polymerization between cross-links and reference ratio is linearly related in synthetic hydrogels. However, the source studies lack the detail and internal validation provided in the current study. The substitution of initial polymer volume fraction for relaxed polymer volume fraction should be further validated by characterization of relaxed polymer volume fractions in multiple systems. To broadly validate fundamental structure-function relationships in hydrogels suggested by the swollen polymer network models, more studies with detailed swelling data collection and reporting are needed.

Modeling molecular weight between cross-links

The average molecular weight between cross-links ($\overline{M}_c$), calculated from swelling data via swollen polymer network models (*9*), estimates the real length of elastically effective chains in a swollen polymer network based on fundamental thermodynamic contributions of polymer-solvent mixing and elastic stretching of network chains. Unlike expected degree of polymerization between cross-links, which represents the ideal case of a homogeneous network without defects, molecular weight between cross-links as it is calculated via swollen polymer network modeling accounts for several chains contributing no elastic energy due to chain-end defects.

Calculating the molecular weight between cross-links requires several system-specific parameters. The relevant values for PVA hydrogels and PEGDA hydrogels are listed in the Supplementary Materials (table S4). The calculations are described in Materials and Methods (Eqs. 12 and 13), and full descriptions of each parameter are available in our recent theoretical review of swollen polymer network models (*9*). Because the reported values for parameters vary greatly (see table S5) and their uncertainty is not reported, error estimates are not included for any values that were calculated using swollen polymer network models.

To evaluate the practical worth of the linear synthesis-swelling relationships and to provide some context for the accuracy of the swollen polymer network models (because error bars are not feasible), expected swelling values based on the linear synthesis-swelling relationships were used as alternative inputs for the swollen polymer network models [i.e., in Figs. 4 (A and B) and 5, the symbols represent calculations based on actual swelling data, and the dotted lines represent calculations based on the linear synthesis-swelling relationships].

The average molecular weight between cross-links was calculated for each formulation of PVA hydrogel and PEGDA hydrogel (Fig. 4, A and B). Both PVA hydrogels and PEGDA hydrogels showed increasing molecular weight between cross-links with increasing degree of polymerization between cross-links, and the rate at which molecular weight between cross-links increased with respect to expected degree of polymerization between cross-links decreased as the initial polymer volume fraction increased. Synthesis- and swelling-based predictions closely matched in PVA and PEGDA hydrogels, except at high degrees of polymerization between cross-links in PEGDA hydrogels, consistent with the variability observed in Fig. 2D.

The solid black lines in Fig. 4 (A and B) represent the ideal relationship between the expected degree of polymerization between cross-links and molecular weight between cross-links, based on a repeating unit molecular weight of 44 g/mol for both PVA and PEGDA. The 10% PVA formulations ($\varphi_0 = 0.100$) closely matched the ideal relationship, and lower initial polymer volume fractions

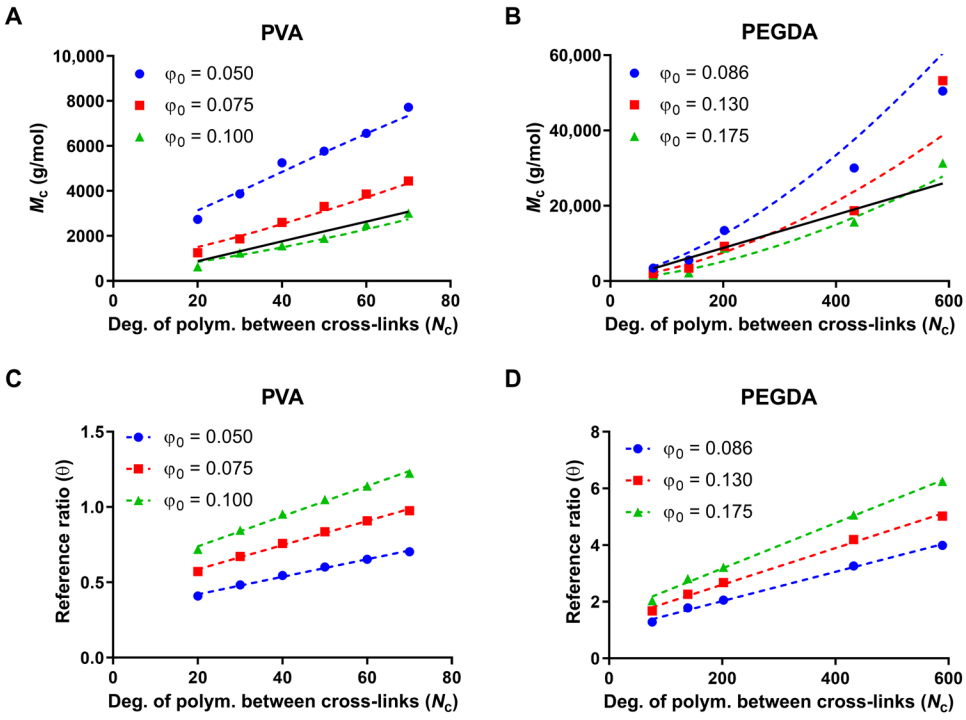

Fig. 4. Expected molecular weight between cross-links and reference ratio calculated with equilibrium swelling theory. Expected molecular weight between cross-links ($\overline{M}_c$) for each formulation of (**A**) PVA hydrogels and (**B**) PEGDA hydrogels. Data were grouped by expected degree of polymerization between cross-links (N_c) and initial polymer volume fraction (φ_0). For (A) and (B), symbols represent predictions based on swelling data, and dotted lines represent predictions based on linear synthesis-swelling relationships. The solid black line represents the ideal molecular weight between cross-links based on the expected degree of polymerization between cross-links, assuming a molecular weight per repeating unit of 44 g/mol for both PVA hydrogels and PEGDA hydrogels. The equilibrium swelling model was inverted to predict the reference ratio based on initial polymer volume fraction and degree of polymerization to demonstrate discrepancies with experimental data on (**C**) PVA hydrogels and (**D**) PEGDA hydrogels. For (C) and (D), dotted lines represent best-fit lines. Fitting parameters are provided in the Supplementary Materials (table S3).

shifted toward higher molecular weights between cross-linking, possibly suggesting that low initial polymer volume fractions reduce the efficiency of the cross-linking reaction.

For the PEGDA formulations, a similar trend between initial polymer volume fraction and cross-linking efficiency is apparent, but with increased separation between formulations at higher degrees of polymerization between cross-links. This result might suggest that the end-linking reaction scheme markedly loses efficiency at high degrees of polymerization between cross-links because of excessive steric hindrance, but this effect cannot be confirmed through comparison with PVA hydrogels because the degrees of polymerization between cross-links of the PEGDA hydrogels far exceeded the degrees of polymerization between cross-links of the PVA hydrogels. The same effect might be observed at high degrees of polymerization between cross-links ($N_c > 100$) for PVA hydrogels. Furthermore, PEGDA formulations at low degrees of polymerization between cross-links had model-estimated molecular weights between cross-links below the ideal relationship, suggesting that some aspect of the swollen polymer network model is flawed in application to PEGDA hydrogels because network defects should only increase molecular weight between cross-links above the ideal value. The analysis of molecular weight between cross-links in PVA hydrogels and PEGDA hydrogels suggests that the way the network structure deviates from ideality may be associated with the reaction scheme used to form the hydrogel, but further studies are needed to clarify those effects. For example, measurement of the fraction of junctions that result in primary loops (*25*) or redundant connections (*26*) might reveal dependencies on the reaction scheme, initial polymer volume fraction, or expected degree of cross-linking that are not considered within the swollen polymer network model. Such defects would reduce the number of elastically effective chains or, as described by Chassé *et al.* (*26*), reduce the effective junction functionality, which is currently treated as an ideal value. Overall, the results validate previous arguments (*27*, *28*) that the modeled molecular weight between cross-links of a hydrogel system is sensitive to both the initial polymer volume fraction and the expected degree of polymerization between cross-links, although the molecular weight between cross-links of an ideal hydrogel would only be affected by the expected degree of polymerization between cross-links.

The modeling analysis described above assumed that the swollen polymer network model is fundamentally correct and fully applicable to real PVA and PEGDA hydrogels. However, the experimental data indicate a strong linear relationship between degree of polymerization between cross-links and the reference ratio that is independent of the initial polymer volume fraction. The mixing component of the modeled relationship scales with the equilibrium-swollen polymer volume fraction, suggesting that the experimentally observed linear independent relationship is not possible. To demonstrate this model-experiment inconsistency, we modeled reference ratio as a function of relaxed polymer volume fraction and molecular weight between cross-links according to the model, where relaxed polymer volume fraction was calculated from the initial polymer volume

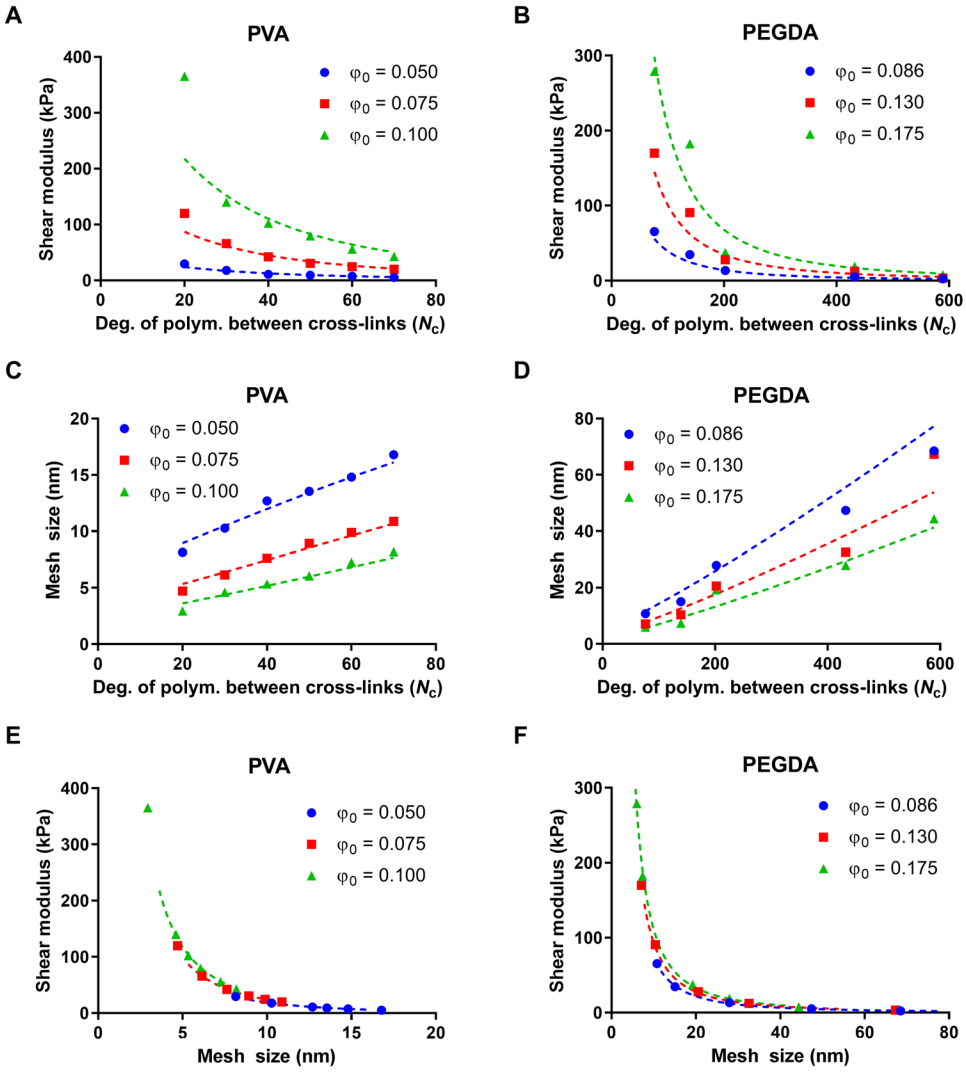

Fig. 5. Expected relationships between synthesis conditions, shear modulus, and mesh size for each formulation of PVA hydrogels and PEGDA hydrogels. Data were grouped by expected degree of polymerization between cross-links (N_c) and initial polymer volume fraction (φ_0). Symbols represent predictions based on swelling data, and dotted lines represent predictions based on linear synthesis-swelling relationships. Shear modulus decreased with increasing degree of polymerization between cross-links in (**A**) PVA hydrogels and (**B**) PEGDA hydrogels. Mesh size increased with degree of polymerization between cross-links in (**C**) PVA hydrogels and (**D**) PEGDA hydrogels. Formulations were predicted to fit along a master inverse curve relating shear modulus and mesh size in (**E**) PVA hydrogels and (**F**) PEGDA hydrogels.

fraction and molecular weight between cross-links was estimated directly from the expected degree of polymerization between cross-links (Fig. 4, C and D). The contrast between experimental results in Fig. 2 (C and D) and modeled results in Fig. 4 (C and D) provides unprecedented insight on the fundamental limitations of equilibrium swelling theory. Where the experimental values are collinear and independent of the initial polymer volume fractions, the modeled values differ in both slope and intersect with response to the initial polymer volume fraction (slope, intersect, and R^2 values provided in table S3). Furthermore, no manipulation of parameter values, such as changing the polymer-solvent interaction parameter, was sufficient to force collinearity and volume fraction independence within the modeled data. Algebraically, the dependence on the relaxed polymer volume fraction could not be eliminated from the model, suggesting that it is conceptually associated with the balance between mixing and elastic energies from Flory-Huggins mixing theory and rubberlike elasticity theory. Together, these results suggest that the mixing-elasticity balance of equilibrium swelling theory does not match experimental data from simple real swollen network systems, and further theoretical development should consider the independent role of the reference ratio as it relates to the molecular weight between cross-links.

Structural relationship between shear modulus and mesh size

From the model-estimated molecular weight between cross-links, both shear modulus and mesh size were estimated for each hydrogel formulation (Fig. 5; Eqs. 14 and 15). For PVA hydrogels and PEGDA hydrogels, estimated shear modulus increased with initial polymer volume fraction and decreased with an inverse response to increasing degree of polymerization between cross-links (Fig. 5, A and B). Synthesis-based predictions and swelling-based predictions closely

agreed, although the synthesis-based predictions systematically underestimated shear modulus at low degrees of polymerization between cross-links, which may be theoretically interpreted as the result of extensive cross-linking nonlinearly disrupting swelling and shear modulus behavior (*20*, *21*). Because of the inverse relationship between degree of polymerization between cross-links and shear modulus, small swelling deviations at low degrees of polymerization create large deviations in the estimated shear modulus. Predicted shear moduli for PVA hydrogels ranged from 5 to 365 kPa, and predicted shear moduli for PEGDA hydrogels ranged from 2 to 279 kPa. Together, these results suggest that adjusting initial polymer volume fraction and expected degree of polymerization between cross-links when designing synthetic hydrogels should facilitate precise control of hydrogel shear modulus over two orders of magnitude.

The estimated mesh size for each system scaled similarly to the molecular weight between cross-links (Fig. 5, C and D). As with shear modulus, PVA hydrogels and PEGDA hydrogels were highly consistent between synthesis-based predictions and swelling-based predictions of mesh size, indicating that diffusivity of solutes in synthetic hydrogels should be highly controllable by manipulating expected degree of polymerization between cross-links and initial polymer volume fraction. PVA hydrogel mesh sizes ranged from 3 to 17 nm, and PEGDA hydrogel mesh sizes ranged from 6 to 69 nm, which should allow either hydrogel system to control the diffusivity of bioactive solutes with comparable hydrodynamic radii such as cytokines and growth factors. The predicted relationships between initial polymer volume fraction, expected degree of polymerization between cross-links, and mesh size agree with previous experimental results described by Jimenez-Vergara *et al.* (*15*) and Cruise *et al.* (*29*).

Changing initial polymer volume fraction and expected degree of polymerization between cross-links affects both estimated shear modulus and estimated mesh size, implying that shear modulus and mesh size are closely correlated. To visualize their relationship, shear modulus was plotted against mesh size for each hydrogel formulation (Fig. 5, E and F). For both polymer systems, predictions of shear modulus and mesh size were collinear for all formulations, effectively creating a master curve. Browning *et al.* (*28*) and Munoz-Pinto *et al.* (*27*) reported a similar master curve from experimental data on PEGDA and mPEG hydrogels. Two important properties result from the master curves. First, the initial polymer volume fraction and the expected degree of polymerization between cross-links hierarchically affect hydrogel physical properties. The initial polymer volume fraction can be used as a coarse control method, shifting along the shear modulus–mesh size curve in relatively large steps, with increasing initial polymer volume fraction favoring higher shear modulus and lower mesh size. The degree of polymerization between cross-links facilitates more precise changes over a smaller range within the curve. Second, the relationship between stiffness and mesh size, though it follows the same inverse form for PVA hydrogels and PEGDA hydrogels, is characteristic of the hydrogel system. Although PVA and PEGDA formulations vary comparably over shear modulus, the PEGDA hydrogels exhibit much broader variation in mesh size. The differences between the curves arise from the unique parameters for each hydrogel system (table S4), which therefore provide further means for either tuning each hydrogel system or selecting the most appropriate system for the study. For example, a PVA hydrogel could be made less restrictive to solutes by decreasing the initial polymer volume fraction and increasing the degree of polymerization between cross-links, but a PEGDA hydrogel could achieve high solute diffusivity more easily if the alcohol side groups in the PVA hydrogel are not chemically relevant.

Ultimately, the master curves describe the limitations of controlling hydrogel physical properties by manipulating initial polymer volume fraction and degree of polymerization between cross-links. Using only these two synthetic handles, shear modulus and mesh size are inseparable properties in biomedical hydrogels, leaving many desirable combinations of physical and chemical properties unattainable. For example, a hydrogel with the chemical properties of PEGDA, a shear modulus of 200 kPa, and a mesh size of 60 nm may be theoretically ideal for a drug-releasing implant but may not be synthetically feasible. Addition of secondary reactive species (*27*) and incorporation of dual polymer networks (*30*) have been proposed as means to independently tune shear modulus and mesh size, but such changes also change chemical properties in the hydrogel. Further insightful studies in hydrogel design are needed to establish robust methods for independently tuning stiffness and solute diffusivity in hydrogels. Sufficiently robust, polymer-independent methods with broad applicability across hydrogel systems would accelerate targeted hydrogel design for biomedical applications.

Limited control of network structure in gelatin-based hydrogels

Having established linear synthesis-swelling relationships in synthetic hydrogels that revealed structural insights into their stiffness-diffusivity relationships, we investigated whether the relationships observed in PVA hydrogels and PEGDA hydrogels could be replicated in a biopolymer hydrogel system of gelatin methacrylamide (GelMA). GelMA hydrogels were selected for their frequent use in biomedical applications (*31*) and because they are covalently cross-linked via photoinitiated methacrylamide polymerization, which allows control of the degree of polymerization between cross-links by varying the extent of methacrylamide functionalization (*14*). GelMA hydrogels were synthesized with a matrix of initial polymer volume fractions and degrees of polymerization between cross-links (table S6) and subject to the same analysis as the PVA hydrogels and PEGDA hydrogels (Fig. 6 and fig. S2). However, several differences between GelMA hydrogels and synthetic hydrogels were expected to limit applicability of the swollen polymer network model. As a biopolymer derived from native tissue, GelMA has greater batch-to-batch variability than synthetic polymers in both molecular weight distribution and repeating unit (amino acid) variations (*14*). Further adding to the complexity is the presence of two major configurations of gelatin, the random coil and the α helix, which are sensitive to temperature, pH, and solvent (*32*, *33*). These can create additional higher-order structures of coiled-helix or triple helix associations, driven by hydrophobic and hydrophilic interactions, hydrogen bonding, and presentation of side groups by the diverse range of amino acids (*34*, *35*). Gelatin random coil and helix configurations are thermoreversible, with coils dominating at elevated temperatures (>30°C) and helices at lower temperatures (*34*, *36*). As such, the swelling studies at room temperature probed the helix-dominated GelMA configuration, a higher-order structure that can lead to physical entanglements and long-range interactions that introduce increased variability compared to PVA and PEGDA systems. In addition to the structural differences, GelMA is more expensive and time-intensive to produce and characterize than PVA and PEGDA, which resulted

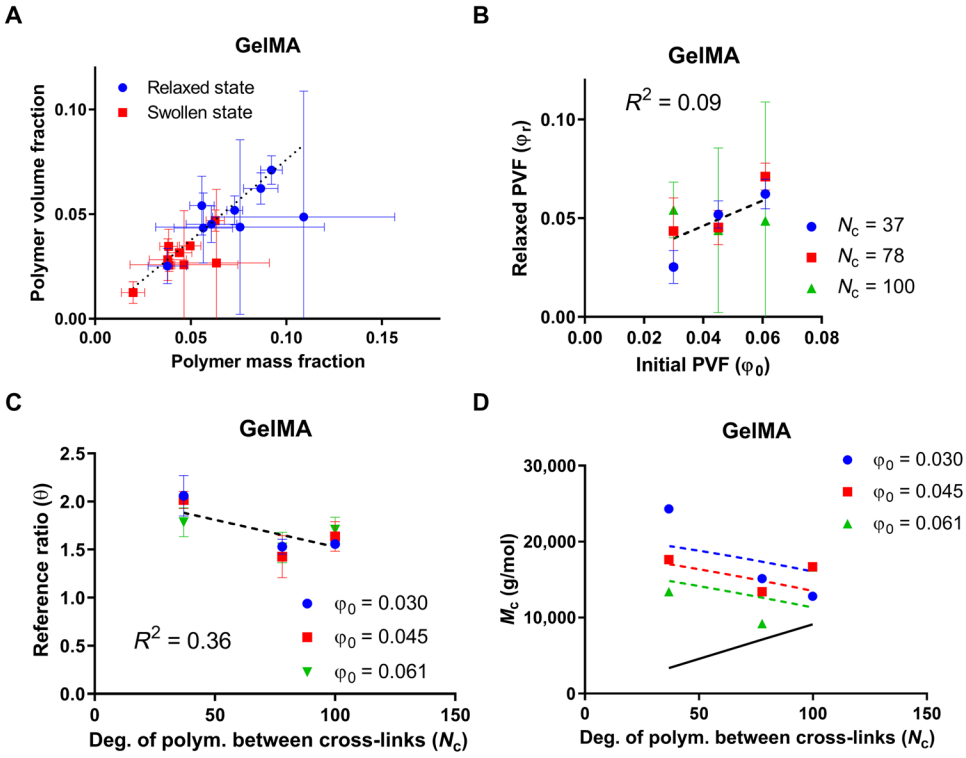

Fig. 6. Replication of the synthesis-swelling studies on GelMA hydrogels did not yield similar linear synthesis-swelling correlations. (**A**) Correlation between mass-based and buoyancy-based polymer volume fraction measurements was unreliable, indicated by the large SDs ($n = 4$) and deviance from the predicted relationship (the dotted line; $\rho_{p,\,GelMA} = 1.35$ g/cm^3, $\rho_w = 1.00$ g/cm^3). (**B**) Relationship between initial polymer volume fraction (φ_0) and relaxed polymer volume fraction (φ_r) in GelMA hydrogels ($n = 4$), with the dotted line and R^2 value describing the overall fit. (**C**) Relationship between the expected degree of polymerization between cross-links (N_c) and reference ratio (θ) in GelMA hydrogels ($n = 4$). (**D**) Expected molecular weight between cross-links ($\overline{M}_c$) for each formulation of GelMA hydrogels. Symbols represent predictions based on swelling data, and dotted lines represent predictions based on linear fits of the synthesis-swelling relationships. The solid black line represents the ideal molecular weight between cross-links based on the expected degree of polymerization between cross-links, assuming an average molecular weight per amino acid of 91.2 g/mol.

in both fewer and smaller samples as compared to the synthetic hydrogels (34 total 5-mm GelMA samples, 103 total 18-mm PVA samples, and 180 total 18-mm PEGDA samples). These sampling differences confounded analysis of the GelMA samples and limit direct comparison between the synthetic hydrogels and the biopolymer hydrogel.

The comparison of polymer volume fraction measured by the mass-based method and the buoyancy-based method (Fig. 6A) had much greater SD per formulation and deviance from the ideal mass-volume relationship [using an average density value of 1.35 g/cm^3 for GelMA (*14*)] than PVA hydrogels and PEGDA hydrogels. The average measured dry density for GelMA samples was 1.27 ± 0.64 g/cm^3 ($n = 34$). These results are consistent with the understanding that GelMA hydrogels have high intrinsic variability based on amino acid variability and higher-order interactions such as intra-chain hydrogen bonding. Unlike with PVA hydrogels and PEGDA hydrogels, the mass-based calculation is not a viable method for accurately measuring the polymer volume fraction of GelMA hydrogels, emphasizing the need for highly accurate buoyancy-based methods for biopolymer systems.

GelMA hydrogels did not display strong linear relationships between synthesis conditions and swelling characteristics (Fig. 6, B and C). The initial polymer volume fraction to relaxed polymer volume fraction relationship was weakened by high variability in the relaxed polymer volume fraction data ($\varphi_r = 0.64\varphi_0 + 0.0206$, $R^2 = 0.09$), and the linear fit of expected degree of polymerization between cross-links to reference ratio resulted, unexpectedly, in a negative slope ($\theta = -0.0056 * N_c + 2.09$, $R^2 = 0.38$). We hypothesize that the GelMA hydrogels, unlike the synthetic hydrogels whose dependence on degree of polymerization between cross-links is primarily associated with the entropic spring model, are highly affected by physical entanglements and intrachain hydrogel bonding (*34*, *35*). Therefore, reference ratio in GelMA hydrogels can be interpreted as a balance between covalent cross-links and physical entanglements (*37*–*39*). This relationship could be further investigated by observing trends at higher temperatures (>30°C) when physical entanglements (helices) are mitigated and chemical cross-links dominate (*36*).

We further analyzed the GelMA hydrogels through the swollen polymer network model to estimate molecular weight between cross-links (Fig. 6D) as well as shear modulus and mesh size (fig. S2). Although we find a similar master curve relating shear modulus and mesh size (fig. S2C), the nature of GelMA hydrogels breaks many of the modeling assumptions included in the current swollen polymer network models (such as having a consistent number of ionic groups per polymeric repeating unit), making further interpretation unreliable (*9*). Notably, the estimated molecular weight between cross-links decreased with increasing degree of polymerization between cross-links, which is likely a result of the physical entanglements acting as pseudo–cross-links as described in the comparison

between expected degree of polymerization between cross-links and reference ratio. This inverse trend is possibly linked to increasing methacrylamide functionalization leading to a decrease in available gelatin conformation states, but further studies would be needed to produce a realistic mechanistic model. Together, the results of our synthesis-swelling analysis and modeling on GelMA hydrogels indicate that larger datasets must be collected for biopolymer hydrogels to account for their natural variability, and more advanced models are needed for biopolymer hydrogels to account for the greater complexity of physical interactions governing their structure-function relationships.

With this study, we demonstrated unprecedented control and cross-system comparison of hydrogel structure and swelling behavior. Simultaneous analysis of hydrogel swelling using mass-based measurements and buoyancy-based measurements validated the use of mass-based measurements in well-characterized synthetic hydrogels and demonstrated the importance of buoyancy-based measurements in conditions where polymer density is unreliable. For PVA hydrogels and PEGDA hydrogels, structural analysis of synthesis conditions revealed two linear, independent relationships between synthesis conditions (initial polymer volume fraction and expected degree of polymerization between cross-links) and swelling behavior (relaxed polymer volume fraction and reference ratio). Further analysis through swollen polymer network models showed that stiffness and solute diffusivity in hydrogels are fundamentally coupled to each other through swollen polymer network structure, which can be precisely manipulated by synthesis conditions. Equivalent studies on GelMA hydrogels demonstrated that more advanced models and context-specific experiments will be needed to precisely control physical properties in biopolymer hydrogels. We anticipate that the combined ease of performing accurate swelling measurements and the associated ability to predict hydrogel physical properties from swelling data, as demonstrated in this work, will motivate more consistent collection and reporting of hydrogel swelling in future studies. Further fundamental model-driven analysis of structure-function relationships in hydrogels will accelerate the process of hydrogel design for biomedical applications.

MATERIALS AND METHODS

Materials

All materials were purchased from Sigma-Aldrich or Thermo Fisher Scientific and used without further purification unless specified otherwise.

Preparation of PVA hydrogels

Eighteen PVA hydrogel formulations were synthesized from PVA of varying concentrations (5, 7.5, and 10 volume percent) and cross-linking ratios (40, 60, 80, 100, 120, or 140 mol PVA repeating unit per mol glutaraldehyde). PVA hydrogels were synthesized as previously described (*18*). Briefly, PVA [M_n = 33884, PDI (polydispersity index) = 1.81; measured with aqueous gel permeation chromatography by EAG Laboratories, Maryland Heights, MO] was dissolved in deionized (DI) water in a 90°C oven overnight (8 to 16 hours) without stirring. Solutions were titrated to pH 1.5 with a minimal volume (1 to 3 ml) of 6 N hydrochloric acid. Glutaraldehyde (25% v/v in DI water) was added to the desired molar ratio. Immediately following the introduction of glutaraldehyde, each solution was rapidly stirred and poured into an 8″ × 3″ Sigmacote-coated glass mold, covered to prevent evaporation, and incubated for 3 hours to allow the cross-linking reaction to proceed. Samples were then cut from the films with biopsy punches (18 mm diameter) and used for swelling analysis.

PEG molecular weight characterization

Before PEGDA synthesis, PEG number-average molecular weights (nominal molecular weights of 3.4, 6, 10, 20, and 35 kDa) were measured via size exclusion chromatography (SEC) carried out on an Agilent system with a 1260 Infinity isocratic pump, degasser, and thermostat column chamber containing a guard column (table S2). Specimens were dissolved in chloroform (2 to 6 mg/ml) at room temperature and syringe-filtered. Injections (100 μl) were passed through an Agilent 5-μm MIXED-D column with an operating range of 200 to 400,000 g mol^{-1} at a flow rate of 0.5 ml/min at 30°C and a mobile phase of chloroform with 50 ppm (parts per million) amylene. Separated components were passed through the Agilent 1260 Infinity refractometer and Agilent 1260 Infinity bio-inert multidetector suite with dual angle static and dynamic light scattering detectors. Number-average molecular weight (M_n) was determined using the Agilent Bio-SEC software relative to PEG standards. For each molecular weight of PEG, three samples were measured with duplicate injections, and the number-average molecular weight was calculated from each measurement (n = 6).

PEGDA synthesis

PEGDA was prepared as previously described (*28*). Briefly, triethylamine (2 molar equivalents) was added dropwise to a solution of PEG (3.4, 6, 10, 20, or 35 kDa) in anhydrous dichloromethane under nitrogen. Acryloyl chloride (4 molar equivalents) was added dropwise. The reaction was allowed to proceed for 24 hours and then quenched with an aqueous solution of sodium bicarbonate (8 molar equivalents). The product was dried with sodium sulfate, precipitated in ice-cold diethyl ether, and then filtered and dried at atmospheric pressure for 24 hours and under vacuum briefly. Successful synthesis was confirmed with proton nuclear magnetic resonance spectroscopy (^{1}H NMR) with a Varian MR 400-MHz spectrometer using a trimethylsilane/solvent signal internal reference. ^{1}H NMR ($CDCl_3$): 3.6 ppm (m, -OCH2CH2-); 6.5 ppm (s, -CH2-NH-); 6.4 ppm (m, -CH=CH2); 5.6 and 6.1 ppm (m, -CH=CH2). Polymers with greater than 85% acrylation were used in this investigation.

Preparation of PEGDA hydrogels

Fifteen PEGDA hydrogel formulations were synthesized from PEGDA of varying molecular weights (3.4, 6, 10, 20, or 35 kDa) at three concentrations [10, 15, or 20 weight % (wt %)]. PEGDA was dissolved in DI water, and the photoinitiator Irgacure 2959 (10 wt % solution in 70% ethanol) was added to 0.1 wt % final solution volume. Precursor solutions were mixed then pipetted between 1.5-mm spaced plates and cross-linked with exposure to longwave 4 mW/cm^2 ultraviolet (UV) light for 6 min on both sides (Ultraviolet Products High-Performance UV Transilluminator; 365 nm; Analytik Jena). Samples were then extracted from the films with biopsy punches (18 mm diameter) and used for swelling analysis.

GelMA synthesis

Porcine Type A gelatin (#G2500, Sigma-Aldrich, St. Louis, MO) was functionalized along its backbone with pendant methacrylamide groups as previously described (*40*). Briefly, methacrylate anhydride was added dropwise to a rapidly stirring solution of gelatin in

phosphate-buffered saline (PBS; 1 g/100 ml) heated to 50°C. The ratio of gelatin to methacrylate anhydride was tuned to control the extent of functionalization of methacrylamide groups on free amines (present in lysine groups along the gelatin backbone) (35, 45, and 95% functionalization; quantified by ^{1}H NMR) (*40*). After reacting for 1 hour, the solution was quenched with 500-ml warm PBS and transferred to dialysis tubing for 7 days of purification, followed by lyophilization until dehydrated.

Preparation of GelMA hydrogels

Nine GelMA hydrogel formulations were synthesized from three concentrations of GelMA (4, 6, and 8 wt %) and three extents of methacrylamide functionalization (35, 45, or 95%). GelMA was dissolved in PBS containing 0.1 wt % lithium acylphosphinate. For each sample, 40 μl of suspension was placed in a circular Teflon mold (5 mm diameter) and cross-linked with exposure to 7.14 mW/cm^2 UV light for 30 s (AccuCure ULM-3 Spot, 365 nm, Digital Light Lab).

Calculation of generalized structural synthesis variables

To compare results across hydrogel systems, generalized synthesis variables were used to describe hydrogel formulations. Instead of initial concentration of polymer in solvent, often reported as either a weight-volume fraction or a weight-weight fraction, initial polymer volume fractions (φ_0) were estimated using known polymer and water densities ($\rho_{p,\,PVA}$ = 1.27 g/cm^3, $\rho_{p,\,PEGDA}$ = 1.18 g/cm^3, $\rho_{p,\,GelMA}$ = 1.35 g/cm^3, ρ_w = 1.00 g/cm^3) according to Eq. 2, where m_p is the polymer mass and m_w is the mass of water (Eq. 1)

$$\varphi_0 = \frac{1}{1 + \frac{\rho_p}{\rho_w}\frac{m_w}{m_p}} \tag{1}$$

The expected degree of polymerization between cross-link calculation followed one of three cases based upon the cross-linking scheme (Eq. 2).

(A) For hydrogels formed from the random cross-linking of existing polymer chains such as PVA hydrogels or radical chain polymerization with a low frequency of multifunctional monomers capable of cross-linking such as PAAm hydrogels, the expected degree of polymerization between cross-links was defined as the moles of polymer repeating unit in the precursor solution divided by the moles of the cross-linking agent or cross-linking monomer with a correction factor for the functionality of the junctions.

(B) For hydrogels formed via end-linking of polymer chains, such as with PEGDA hydrogels and PEGDMA hydrogels, expected degree of polymerization between cross-links was defined as the number-average molecular weight of the precursor polymer divided by the molecular weight of the polymer's repeating unit.

(C) For GelMA hydrogels wherein cross-linking is defined by the presence of methacrylamide functional groups, the expected degree of polymerization between cross-links was estimated by the inverse frequency of methacrylamide-functionalized amino acids

$$N_c = \begin{cases} \dfrac{2 * \text{moles polymer repeating unit}}{f * \text{moles cross-linking agent}} & \text{(A)} \\ \dfrac{\text{MW precursor polymer}}{\text{MW repeating unit}} & \text{(B)} \\ \dfrac{1}{\text{Frequency of methacrylamide groups}} & \text{(C)} \end{cases} \tag{2}$$

Volumetric swelling characterization

For all swelling samples, three volumetric measurements were performed in series following cross-linking. All samples were first measured immediately following synthesis (relaxed state). Samples were then swollen to equilibrium in either PBS (PVA and GelMA) or DI water (PEGDA) and measured again (swollen state). PBS-swollen samples were then desalted by solvent exchange with DI water. Samples were dried under vacuum (PVA, 40°C; GelMA, 30°C; PEGDA, room temperature) before a final measurement (dry state).

For each volumetric measurement, hydrogel samples were weighed both in air and while suspended in heptane or hexane (nonpolar organic solvents that are insoluble with water and most hydrogel polymers). The difference between a sample's mass (m) and apparent mass (m') when suspended in the nonsolvent ($\rho_{ns,\,hept}$ = 0.6635 g/cm^3, $\rho_{ns,\,hex}$ = 0.6928 g/cm^3) was used to determine the sample's volume in each condition (Eq. 3). Before each measurement, samples were superficially wiped dry to remove any unbound water

$$V = \frac{m - m'}{\rho_{ns}} \tag{3}$$

To facilitate accessibility of the buoyancy-based method for analyzing polymer volume fraction, 3D-printed density kits were designed and manufactured. STL object files for all the 3D-printed parts are available online (www.thingiverse.com/thing:3972888). For this study, density kits were printed using poly(lactic acid) on a CraftBot+ printer (Craftunique Ltd., Budapest, Hungary).

For all datasets, swelling behavior was quantified as the relaxed polymer volume fraction and the reference ratio. When buoyancy-based volumetric measurements were used, relaxed polymer volume fraction (φ_r), swollen polymer volume fraction (φ_s), and reference ratio (θ) were calculated on the basis of the relaxed volume (V_r), the swollen volume (V_s), and the dry volume (V_d) (Eqs. 4 to 6)

$$\varphi_r = \frac{V_d}{V_r} \tag{4}$$

$$\varphi_s = \frac{V_d}{V_s} \tag{5}$$

$$\theta = \frac{\varphi_r}{\varphi_s} \tag{6}$$

The buoyancy-based volumetric measurement enabled independent measurement of the dry density of the polymer network (Eq. 7)

$$\rho_d = \frac{m_d}{V_d} \tag{7}$$

For comparison with buoyancy-based measurements, polymer volume fraction was estimated from the relaxed polymer mass fraction (ψ_r), the swollen polymer mass fraction (ψ_s), and polymer and water densities (Eqs. 8 to 11)

$$\psi_r = \frac{m_d}{m_r} \tag{8}$$

$$\psi_s = \frac{m_d}{m_s} \tag{9}$$

$$\varphi_r = \frac{1}{1 + \frac{\rho_p}{\rho_w}\left(\frac{1}{\psi_r} - 1\right)} \tag{10}$$

$$\varphi_s = \frac{1}{1 + \frac{\rho_p}{\rho_w}\left(\frac{1}{\psi_s} - 1\right)} \tag{11}$$

Swollen polymer network modeling calculations

Thermodynamic equations were used to predict hydrogel structural and physical properties. All parameters used for predictive modeling calculations are provided in table S4, with short descriptions of the parameters in table S5 and further details explaining each parameter available in our recent fundamental modeling review (*9*). The equilibrium swelling equation (Eq. 12) was used to determine the effective molecular weight between cross-links ($\overline{M}_c$) for each hydrogel formulation

$$\frac{1}{\overline{M}_c} = \frac{\ln(1-\varphi_s)+\varphi_s+\chi\varphi_s^2}{-1*\left(1-\frac{2}{f}\right)(1-\gamma)V_1\rho_p\varphi_r^{\frac{2}{3}}\varphi_s^{\frac{1}{3}}} \quad (12)$$

The functionality of PVA hydrogels was expected to be four based on glutaraldehyde acting as a small-molecule cross-linking agent at random points along PVA chains. Because PEGDA and GelMA hydrogels are both radically cross-linked, their functionality (*f*) is unknown. For GelMA hydrogels, the junction functionality was expected to be four in most cases, because cross-linking two chains together is likely to create large amounts of local steric hindrance, preventing further cross-linking. For PEGDA hydrogels, steric hindrance may have a smaller effect because the polymer chains are end-linked rather than cross-linked, enabling higher-functionality junctions. Furthermore, previous studies using PEGDA and PEG acrylate suggest that the degree of acrylate group polymerization likely exceeds 100 for hydrogel-like synthesis conditions (*13*). Therefore, the functionality of PEGDA hydrogels was treated as infinity (*13*), allowing it to be algebraically eliminated from the predictive modeling equations. This simplification is fundamentally defensible because the effect of functionality on molecular weight between cross-links quickly approaches an asymptotic limit as functionality increases (*9*).

For PVA and GelMA hydrogels, the frequency of chain-end defects (γ) was also calculated by substituting a polymer molecular weight–based correction (Eq. 13) into Eq. 12. For PEGDA hydrogels, the frequency of chain-end defects was estimated on the basis of the extent of acrylate functionalization of PEG molecules. Under the simplifying assumptions that all instances of incomplete functionalization resulted in PEG acrylate molecules and all acrylate groups react into the network structure [previous studies suggest 78 to 100% conversion of acrylates with increasing conversion as polymer concentrations increases (*13*)], the frequency of chain-end defects was calculated by subtracting the extent of functionalization from unity

$$\gamma = \frac{f\overline{M}_c}{(f-2)\overline{M}_n} \quad (13)$$

From knowledge of the effective molecular weight between cross-links and hydrogel swelling, shear modulus (*G*) was calculated according to rubberlike elasticity theory (Eq. 14)

$$G = \mathrm{RT}\left(1-\frac{2}{f}\right)(1-\gamma)\frac{\rho_p}{\overline{M}_c}\varphi_r^{\frac{2}{3}}\varphi_s^{\frac{1}{3}} \quad (14)$$

Mesh size for each formulation was calculated using a modified Canal-Peppas relationship that accounts for the effect of junction functionality and nonvinyl polymer repeating units (Eq. 15)

$$\xi = \varphi_s^{-\frac{1}{3}}\left(\left(1-\frac{2}{f}\right)\bar{l}^2 C_\infty\frac{\lambda\overline{M}_c}{M_r}\right)^{\frac{1}{2}} \quad (15)$$

For calculations based on linear synthesis-swelling relationships, the linear prediction of φ_r based on φ_r and θ as a function of N_c were substituted into the predictive calculations, with the swollen polymer volume fraction evaluated as $\varphi_s = \frac{\varphi_r}{\theta}$ (see Eq. 6).

Statistical analysis

Please refer to the figure legends or the relevant sections of Materials and Methods for description of sample size and statistical details. Each experiment was repeated in triplicate or more ($n \geq 3$). Data are displayed as means ± SD. Statistical analysis was performed with Prism 6 (GraphPad Software, La Jolla, USA), and R^2 values >0.9 and *P* values <0.05 were considered significant.

SUPPLEMENTARY MATERIALS

Supplementary material for this article is available at http://advances.sciencemag.org/cgi/content/full/7/7/eabe3245/DC1

View/request a protocol for this paper from *Bio-protocol*.

REFERENCES AND NOTES

1. A. Mandal, J. R. Clegg, A. C. Anselmo, S. Mitragotri, Hydrogels in the clinic. *Bioeng. Transl. Med.* **5**, e10158 (2020).
2. N. A. Peppas, D. S. Van Blarcom, Hydrogel-based biosensors and sensing devices for drug delivery. *J. Control. Release* **240**, 142–150 (2016).
3. S. R. Caliari, J. A. Burdick, A practical guide to hydrogels for cell culture. *Nat. Methods* **13**, 405–414 (2016).
4. J. Li, D. J. Mooney, Designing hydrogels for controlled drug delivery. *Nat. Rev. Mater.* **1**, 16071 (2016).
5. D. E. Discher, D. J. Mooney, P. W. Zandstra, Growth factors, matrices, and forces combine and control stem cells. *Science* **324**, 1673–1677 (2009).
6. B. P. Mahadik, N. A. K. Bharadwaj, R. H. Ewoldt, B. A. C. Harley, Regulating dynamic signaling between hematopoietic stem cells and niche cells via a hydrogel matrix. *Biomaterials* **125**, 54–64 (2017).
7. C. Crocini, C. J. Walker, K. S. Anseth, L. A. Leinwand, Three-dimensional encapsulation of adult mouse cardiomyocytes in hydrogels with tunable stiffness. *Prog. Biophys. Mol. Biol.* **154**, 71–79 (2020).
8. E. Axpe, G. Orive, K. Franze, E. A. Appel, Towards brain-tissue-like biomaterials. *Nat. Commun.* **11**, 3423 (2020).
9. N. R. Richbourg, N. A. Peppas, The swollen polymer network hypothesis: Quantitative models of hydrogel swelling, stiffness, and solute transport. *Prog. Polym. Sci.* **105**, 101243 (2020).
10. M. A. English, L. R. Soenksen, R. V. Gayet, H. de Puig, N. M. Angenent-Mari, A. S. Mao, P. Q. Nguyen, J. J. Collins, Programmable CRISPR-responsive smart materials. *Science* **365**, 780–785 (2019).
11. J. Li, R. Xing, S. Bai, X. Yan, Recent advances of self-assembling peptide-based hydrogels for biomedical applications. *Soft Matter* **15**, 1704–1715 (2019).
12. L. J. Macdougall, K. Anseth, Bioerodible hydrogels based on photopolymerized poly(ethylene glycol)-*co*-poly(α-hydroxy acid) diacrylate macromers. *Macromolecules* **53**, 2295–2298 (2020).
13. J. A. Beamish, J. Zhu, K. Kottke-Marchant, R. E. Marchant, The effects of monoacrylated poly(ethylene glycol) on the properties of poly(ethylene glycol) diacrylate hydrogels used for tissue engineering. *J. Biomed. Mater. Res. A* **92**, 441–450 (2010).
14. A. E. Gilchrist, S. Lee, Y. Hu, B. A. C. Harley, Soluble signals and remodeling in a synthetic gelatin-based hematopoietic stem cell niche. *Adv. Healthc. Mater.* **8**, 1900751 (2019).
15. A. C. Jimenez-Vergara, J. Lewis, M. S. Hahn, D. J. Munoz-Pinto, An improved correlation to predict molecular weight between crosslinks based on equilibrium degree of swelling of hydrogel networks. *J. Biomed. Mater. Res. B Appl. Biomater.* **106**, 1339–1348 (2018).
16. C. T. Reinhart, N. A. Peppas, Solute diffusion in swollen membranes. Part II. Influence of crosslinking on diffusive properties. *J. Membr. Sci.* **18**, 227–239 (1984).
17. Y. Liu, N. E. Vrana, P. A. Cahill, G. B. McGuinness, Physically crosslinked composite hydrogels of PVA with natural macromolecules: Structure, mechanical properties, and endothelial cell compatibility. *J. Biomed. Mater. Res. B Appl. Biomater.* **90**, 492–502 (2009).
18. G. B. McKenna, F. Horkay, Effect of crosslinks on the thermodynamics of poly(vinyl alcohol) hydrogels. *Polymer* **35**, 5737–5742 (1994).
19. P.-G. De Gennes, *Scaling Concepts in Polymer Physics* (Cornell Univ. Press, 1979).
20. J. Kovac, Modified Gaussian model for rubber elasticity. *Macromolecules* **11**, 362–365 (1978).
21. N. A. Peppas, H. J. Moynihan, L. M. Lucht, The structure of highly crosslinked poly(2-hydroxyethyl methacrylate) hydrogels. *J. Biomed. Mater. Res.* **19**, 397–411 (1985).

22. T. Canal, N. A. Peppas, Correlation between mesh size and equilibrium degree of swelling of polymeric networks. *J. Biomed. Mater. Res.* **23**, 1183–1193 (1989).
23. F. Horkay, A. M. Hecht, E. Geissler, Effect of cross-links on the swelling equation of state: Polyacrylamide hydrogels. *Macromolecules* **22**, 2007–2009 (1989).
24. L. M. Weber, C. G. Lopez, K. S. Anseth, Effects of PEG hydrogel crosslinking density on protein diffusion and encapsulated islet survival and function. *J. Biomed. Mater. Res. A* **90A**, 720–729 (2009).
25. H. Zhou, J. Woo, A. M. Cok, M. Wang, B. D. Olsen, J. A. Johnson, Counting primary loops in polymer gels. *Proc. Natl. Acad. Sci. U.S.A.* **109**, 19119–19124 (2012).
26. W. Chassé, M. Lang, J.-U. Sommer, K. Saalwächter, Cross-link density estimation of PDMS networks with precise consideration of networks defects. *Macromolecules* **45**, 899–912 (2012).
27. D. J. Munoz-Pinto, S. Samavedi, B. Grigoryan, M. S. Hahn, Impact of secondary reactive species on the apparent decoupling of poly(ethylene glycol) diacrylate hydrogel average mesh size and modulus. *Polymer* **77**, 227–238 (2015).
28. M. B. Browning, T. Wilems, M. Hahn, E. Cosgriff-Hernandez, Compositional control of poly(ethylene glycol) hydrogel modulus independent of mesh size. *J. Biomed. Mater. Res. A* **98A**, 268–273 (2011).
29. G. M. Cruise, D. S. Scharp, J. A. Hubbell, Characterization of permeability and network structure of interfacially photopolymerized poly(ethylene glycol) diacrylate hydrogels. *Biomaterials* **19**, 1287–1294 (1998).
30. C. Cha, S. Y. Kim, L. Cao, H. Kong, Decoupled control of stiffness and permeability with a cell-encapsulating poly(ethylene glycol) dimethacrylate hydrogel. *Biomaterials* **31**, 4864–4871 (2010).
31. K. Yue, G. Trujillo-de Santiago, M. M. Alvarez, A. Tamayol, N. Annabi, A. Khademhosseini, Synthesis, properties, and biomedical applications of gelatin methacryloyl (GelMA) hydrogels. *Biomaterials* **73**, 254–271 (2015).
32. A. H. Clark, S. B. Ross-Murphy, Structural and mechanical properties of biopolymer gels, in *Biopolymers* (Advances in Polymer Science, 1987), pp. 57–192.
33. P. Sajkiewicz, D. Kolbuk, Electrospinning of gelatin for tissue engineering—Molecular conformation as one of the overlooked problems. *J. Biomater. Sci. Polym. Ed.* **25**, 2009–2022 (2014).
34. K. Beck, B. Brodsky, Supercoiled protein motifs: The collagen triple-helix and the alpha-helical coiled coil. *J. Struct. Biol.* **122**, 17–29 (1998).
35. S. Leikin, D. C. Rau, V. A. Parsegian, Temperature-favoured assembly of collagen is driven by hydrophilic not hydrophobic interactions. *Nat. Struct. Biol.* **2**, 205–210 (1995).
36. J. L. Gornall, E. M. Terentjev, Helix–coil transition of gelatin: Helical morphology and stability. *Soft Matter* **4**, 544–549 (2008).
37. A. I. Van Den Bulcke, B. Bogdanov, N. De Rooze, E. H. Schacht, M. Cornelissen, H. Berghmans, Structural and rheological properties of methacrylamide modified gelatin hydrogels. *Biomacromolecules* **1**, 31–38 (2000).
38. L. Rebers, T. Granse, G. E. M. Tovar, A. Southan, K. Borchers, Physical interactions strengthen chemical gelatin methacryloyl gels. *Gels* **5**, 4 (2019).
39. J. A. Deiber, M. L. Ottone, M. V. Piaggio, M. B. Peirotti, Characterization of cross-linked polyampholytic gelatin hydrogels through the rubber elasticity and thermodynamic swelling theories. *Polymer* **50**, 6065–6075 (2009).
40. S. Pedron, B. A. C. Harley, Impact of the biophysical features of a 3D gelatin microenvironment on glioblastoma malignancy. *J. Biomed. Mater. Res. A* **101**, 3404–3415 (2013).
41. N. A. Peppas, S. L. Wright, Drug diffusion and binding in ionizable interpenetrating networks from poly(vinyl alcohol) and poly(acrylic acid). *Eur. J. Pharm. Biopharm.* **46**, 15–29 (1998).
42. A. S. Hickey, N. A. Peppas, Mesh size and diffusive characteristics of semicrystalline poly(vinyl alcohol) membranes prepared by freezing/thawing techniques. *J. Membr. Sci.* **107**, 229–237 (1995).
43. J. Brandrup, E. H. Immergut, E. A. Grulke, A. Abe, D. R. Bloch, *Polymer Handbook* (Wiley, 1989), vol. 7.
44. B. D. Barr-Howell, N. A. Peppas, Importance of junction functionality in highly crosslinked polymers. *Polymer Bull.* **13**, 91–96 (1985).
45. E. W. Merrill, K. A. Dennison, C. Sung, Partitioning and diffusion of solutes in hydrogels of poly(ethylene oxide). *Biomaterials* **14**, 1117–1126 (1993).
46. P. J. Flory, *Statistical Mechanics of Chain Molecules* (Interscience, 1980).
47. H. Lin, T. Kai, B. D. Freeman, S. Kalakkunnath, D. S. Kalika, The effect of cross-linking on gas permeability in cross-linked poly(ethylene glycol diacrylate). *Macromolecules* **38**, 8381–8393 (2005).
48. S. Lee, X. Tong, F. Yang, The effects of varying poly(ethylene glycol) hydrogel crosslinking density and the crosslinking mechanism on protein accumulation in three-dimensional hydrogels. *Acta Biomater.* **10**, 4167–4174 (2014).
49. G. S. Offeddu, E. Axpe, B. A. C. Harley, M. L. Oyen, Relationship between permeability and diffusivity in polyethylene glycol hydrogels. *AIP Adv.* **8**, 105006 (2018).
50. H. B. Bohidar, S. S. Jena, Kinetics of sol–gel transition in thermoreversible gelation of gelatin. *J. Chem. Phys.* **98**, 8970–8977 (1993).
51. R. A. Engh, R. Huber, Accurate bond and angle parameters for x-ray protein structure refinement. *Acta Crystallogr. Sect. A* **47**, 392–400 (1991).
52. C. Özdemir, A. Güner, Solution thermodynamics of poly(ethylene glycol)/water systems. *J. Appl. Polym. Sci.* **101**, 203–216 (2006).
53. U. Akalp, S. Chu, S. C. Skaalure, S. J. Bryant, A. Doostan, F. J. Vernerey, Determination of the polymer-solvent interaction parameter for PEG hydrogels in water: Application of a self learning algorithm. *Polymer* **66**, 135–147 (2015).
54. P. C. Hiemenz, T. P. Lodge, *Polymer Chemistry* (CRC Press, 2007).
55. I. Pezron, M. Djabourov, J. Leblond, Conformation of gelatin chains in aqueous solutions: 1. A light and small-angle neutron scattering study. *Polymer* **32**, 3201–3210 (1991).
56. S. Ma, M. Natoli, X. Liu, M. P. Neubauer, F. M. Watt, A. Fery, W. T. S. Huck, Monodisperse collagen–gelatin beads as potential platforms for 3D cell culturing. *J. Mater. Chem. B* **1**, 5128–5136 (2013).
57. I. G. Fels, Hydration and density of collagen and gelatin. *J. Appl. Polym. Sci.* **8**, 1813–1824 (1964).
58. J. H. Fessler, A. J. Hodge, Ultracentrifugal observation of phase transitions in density gradients. I. The collagen system. The collagen system. *J. Mol. Biol.* **5**, 446–449 (1962).

Acknowledgments: We would like to thank M. Chwatko for molecular weight characterization of PEG precursor samples, J. Sun and A. Ravikumar for assistance in the literature search for the meta-analysis, and S. Salvador for assistance in designing the 3D-printed density kit. We wish to thank an anonymous reviewer for substantial comments and questions that helped to improve and clarify the interpretation and discussion of results. **Funding:** Research reported in this publication was supported by the National Institute of Diabetes and Digestive and Kidney Diseases of the NIH under Award Numbers R01 DK099528 (B.A.C.H.) and F31 DK117514 (A.E.G.), the National Cancer Institute of the NIH under Award Number R01 CA197488 (B.A.C.H.), as well as by the National Institute of Biomedical Imaging and Bioengineering of the NIH under Award Numbers R01 EB022025 (N.A.P.), R21 EB018481 (B.A.C.H.), and T32 EB019944 (A.E.G.). Further support was provided by the NSF under Award Number DGE-1610403 (N.R.R.). The content is solely the responsibility of the authors and does not necessarily represent the official views of the NIH or the NSF. **Author contributions:** N.R.R.: conceptualization, methodology, software, validation, formal analysis, investigation, data curation, writing—original draft, writing—review and editing, visualization, and project administration; M.W.: conceptualization, methodology, validation, investigation, data curation, and writing—review and editing; A.E.G.: methodology, validation, investigation, data curation, and writing—review & editing; S.T.: validation and investigation; B.A.C.H.: resources, writing—review and editing, supervision, and funding acquisition; E.C.-H.: conceptualization, resources, writing—review and editing, supervision, and funding acquisition; N.A.P.: conceptualization, methodology, resources, writing—review and editing, supervision, project administration, and funding acquisition. **Competing interests:** The authors declare that they have no competing interests. **Data and materials availability:** All data needed to evaluate the conclusions in the paper are present in the paper and/or the Supplementary Materials. All the raw data, processed data, R scripts, and GraphPad Prism files for this project are available on Figshare (https://doi.org/10.6084/m9.figshare.c.5010869) or by contacting the corresponding or primary authors.

Submitted 13 August 2020
Accepted 23 December 2020
Published 12 February 2021
10.1126/sciadv.abe3245

Citation: N. R. Richbourg, M. Wancura, A. E. Gilchrist, S. Toubbeh, B. A. C. Harley, E. Cosgriff-Hernandez, N. A. Peppas, Precise control of synthetic hydrogel network structure via linear, independent synthesis-swelling relationships. *Sci. Adv.* **7**, eabe3245 (2021).

ScienceAdvances

Precise control of synthetic hydrogel network structure via linear, independent synthesis-swelling relationships

N. R. Richbourg, M. Wancura, A. E. Gilchrist, S. Toubbeh, B. A. C. Harley, E. Cosgriff-Hernandez, and N. A. Peppas

Sci. Adv., **7** (7), eabe3245.
DOI: 10.1126/sciadv.abe3245

Science Advances (ISSN 2375-2548) is published by the American Association for the Advancement of Science. 1200 New York Avenue NW, Washington, DC 20005. The title *Science Advances* is a registered trademark of AAAS.